RSC Advances

PAPER

View Article Online
View Journal | View Issue

Cite this: *RSC Adv.*, 2019, **9**, 11901

An electrochemical sensor based on poly(procaterol hydrochloride)/carboxyl multi-walled carbon nanotube for the determination of bromhexine hydrochloride†

Dexian Kong, *[a] Libin Han,[a] Zeming Wang,[a] Lili Jiang,[b] Qian Zhang,[a] Qiong Wu,[a] Jinwei Su,[a] Chunhua Lu*[b] and Guonan Chen[b]

Received 15th October 2018
Accepted 25th March 2019

DOI: 10.1039/c8ra08510b

rsc.li/rsc-advances

Poly(procaterol hydrochloride) (p-ProH) polymeric film was successfully deposited onto the carboxyl multi-walled carbon nanotube (CMWCNT) modified glass carbon electrode (GCE) to construct a p-ProH/CMWCNT composite modified GCE. Due to the synergistic effect of p-ProH and CMWCNT in the composite, the developed sensor can enormously enhance the oxidation peak current of bromhexine hydrochloride (BrH) at *ca.* + 0.90 V. Based on this appearance, an electrochemical method was established for the sensitive and selective determination of BrH with differential pulse voltammetry (DPV). Various conditions affecting the peak current response of BrH were studied and optimized. Under the best conditions, the oxidation peak current of BrH is linear to its concentration in two linear dynamic ranges of 0.2–1.0 μmol L^{-1} ($R = 0.9948$) and 1.0–8.0 μmol L^{-1} ($R = 0.9956$), with a detection limit of 0.1 μmol L^{-1} (S/N = 3). Interference experiment indicated that the as-prepared electrochemical sensor showed wonderful selectivity to the recognition of BrH and was free from disturbance of many other electro-active substances such as dopamine, ascorbic and uric acid. Finally, the practicability of the BrH sensor was verified by the satisfactory results acquired from the BrH determination in pharmaceutical preparation and human serum.

1. Introduction

Bromhexine hydrochloride (BrH), which is chemically named 2-amino-3,5-dibromo-*N*-cyclohexyl-*N*-methylbenzylamine hydrochloride (Fig. 1), is clinically applied to the treatment of chronic obstructive pulmonary diseases such as bronchiectasis, chronic bronchitis, and emphysema. BrH could restrain the synthesis of acid glycoprotein and break the mucin fibers in the sputum, thus reducing and diluting the phlegm which consequently facilitates the expectoration of sputum.[1] Despite being widely used, the improper use of BrH may damage the patient's gastric mucosal barrier and it is particularly detrimental to patients with chronic gastric ulcers. Thus the quantitative analysis of BrH is very important in some fields such as clinical chemistry and pharmaceutical production. Various analytical protocols have been developed to determine the BrH content in biological samples, namely UV-visible spectrophotometry,[2–4] high performance liquid chromatography (HPLC) with a UV detector,[5,6] the thin layer chromatography (TLC) densitometric method,[7] capillary isotachophoresis (ITP) with a conductimetric detector,[8] chemiluminescence[9] and electrochemical methods.[10–12] Compared with other methods, the electrochemical technique possesses the merits such as simple apparatus, ease of operation, excellent selectivity and high sensitivity. As far as we know, there are merely three published articles concerning the electrochemical analysis of BrH. Turchán *et al.* has comprehensively studied the electrochemical behavior of BrH in Britton–Robinson buffer solution and developed an electrochemical method to quantify BrH in pharmaceutical preparation with DPV method.[10] Flow injection analysis coupled with amperometric detection (FIA-ED) method for BrH detection was established by Mika *et al.*[11] Kutluay *et al.* fabricated an electrochemical sensor based on nickel nanoparticles functionalized MWCNT at platinum electrode for BrH determination.[12]

Nanomaterials, which have electrical and physical properties that are not available in traditional materials, such as volumetric effects, surface effects, quantum size effects, macroscopic quantum tunneling effects and dielectric confinement effects, have been widely used in optoelectronics,[13] power industry,[14] energy conversion and storage devices,[15] biomedical and environmental protection,[16] electrochemical sensors,[17] *etc.*

[a]*College of Life Sciences, Fujian Agriculture and Forestry University, Fuzhou, Fujian 350002, China. E-mail: dexian_kong@163.com*

[b]*College of Chemistry, Fuzhou University, Fujian, 350108, China. E-mail: chunhualu@fzu.edu.cn*

† Electronic supplementary information (ESI) available. See DOI: 10.1039/c8ra08510b

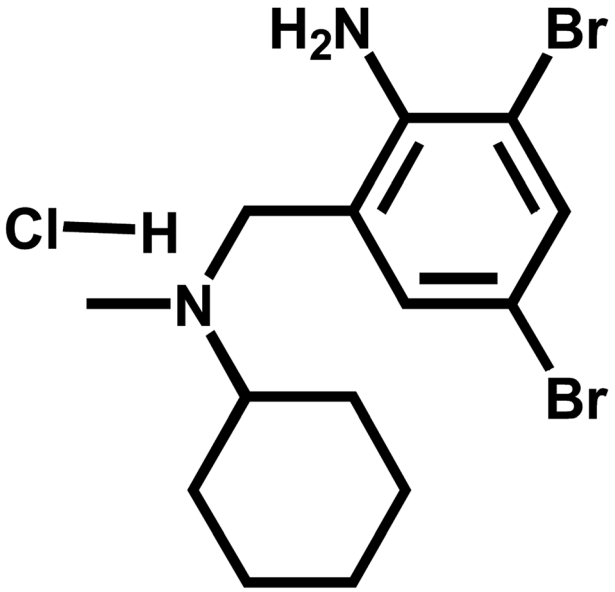

Fig. 1 The chemical structure of BrH.

Owning to the unique electrochemical properties, electropolymerization materials have attracted plenty of attention in the field of electrochemical analysis. Many electropolymerized films, including poly(amino acid), polyaniline, poly(luminol), polypyrrole, polyphenol, *etc.*, or their mixed polymer film have been designed to fabricated electrochemical sensors for selectively and sensitively detecting large amount of biomacromolecules, inorganic and organic molecules.[18–20] The fabrication process of these electropolymerized film modified sensors commonly includes the electropolymerization of electro-active monomers on the electrode surface, which enhances the controllability of the film thickness and reproducibility of the electrochemical sensors. In order to acquire larger electropolymerization surface and better sensitivity, electropolymerized films are usually used in combination with carbon nanomaterials (such as carbon nanotubes (CNT), carbon nanohorns, fullerenes, graphene).[21,22] Among those carbon nanomaterials, CNTs have been most widely used due to their rich pore structures, large specific surface areas, and surface group functionalizable.[23–25] Since the three-dimensional nanostructure of CNT can provide a larger electro-active surface, polymer/CNT composite modified electrodes which hold more ideal electron conduction capability and mechanical strength have been developed and applied to the sensitive and selective analysis of nucleic acid,[26,27] enzyme,[28,29] inorganic ions[30,31] and organic molecules,[32,33] showing out a wide application prospect in analytical chemistry.

Recently, a poly(procaterol hydrochloride) (p-ProH) electropolymerized film modified glass carbon electrode (GCE) was successfully developed by our group.[34] The p-ProH film modified GCE exhibited excellent electron conduction efficiency towards to the oxidation of dopamine and uric acid and was suitable for the simultaneous determination of these two compounds. In this study, p-ProH film was directly electropolymerized onto the carboxyl multi-walled carbon nanotube (CMWCNT) modified glass carbon electrode (GCE) to construct a p-ProH/CMWCNT composite modified GCE. Compared with p-ProH/GCE and CMWCNT/GCE, the oxidation peak current of BrH at p-ProH/CMWCNT composite modified GCE was greatly enhanced. After optimizing several conditions, sensitive and selective determination of BrH was achieved with the developed sensor.

2. Experimental

2.1. Reagents and solutions

Procaterol hydrochloride (ProH) was purchased from National Institute for the Control of Pharmaceutical and Biological Products (Beijing, China). Bromhexine hydrochloride (BrH) was obtained from Shanghai Makclin Biochemical Co., Ltd (Shanghai, China). CMWCNT with ~8 nm outer diameter and 0.5–2 μm length was acquired from Nanjing XFNANO Materials Tech Co., Ltd (Nanjing, China). Polyvinyl alcohol (PVA) powder was supplied by Sinopharm Chemical Reagent Co., Ltd (Shanghai, China). Bromhexine tablets (Marked 8.0 mg bromhexine each tablet) for analytical application were produced by Wanbangde Pharmaceutical Group CO. LTD. Human blood serum was kindly provided by Fujian medical university. All other reagents used were analytical pure and purchased from local suppliers. Stock solution of BrH (0.01 mol L^{-1}) was prepared by dissolving exact mass of BrH powder in methanol and was stored hermetically in the refrigerator. PVA aqueous solution (0.25 wt%) was prepared according to our previous report.[17] Double distilled water was used throughout the experiments.

2.2. Apparatus

All electrochemical experiments were performed on a CHI660E Electrochemical Workstation manufactured by Shanghai Chenhua Instruments (Shanghai, China). Three electrodes system containing a bared or modified GCE working electrode, a platinum wire auxiliary electrode and a saturated Ag/AgCl reference electrode was employed. The morphologies of CMWCNT/GCE and p-ProH/CMWCNT/GCE were studied with a Nova NanoSEM 230 field emission scanning electron microscope (USA).

2.3. Preparation of p-ProH/CMWCNT composite modified GCE

Prior to the fabrication, GCE was rigorously cleaned by means of polished on polishing flannelette with alumina slurries and then sonicated in alcohol and water for 1 min in turns, finally dried in air. 2 mg of CMWCNT was accurately added into mix solution of 0.5 mL PVA and 0.5 mL ethanol, after sonicating 30 min, homogeneous dispersed solution of 2 mg mL^{-1} CMWCNT was obtained. 7.5 μL of the above mentioned CMWCNT dispersion was casted onto the pretreated GCE surface and dried in air to get CMWCNT modified GCE (denoted as CMWCNT/GCE). Then, the CMWCNT/GCE was immersed into a pH 5.5 phosphate buffer solution (PBS) (0.2 mol L^{-1})

containing 5.0×10^{-5} mol L^{-1} ProH, treated by CV scans in the potential range of −0.8–2.0 V with scanning rate of 100 mV s^{-1}, after 6 cycles' scans, p-ProH film was *in situ* deposited onto the surface of CMWCNT/GCE to obtain a p-ProH/CMWCNT composite modified GCE (denoted as p-ProH/CMWCNT/GCE). In order to remove the adsorbed ProH monomer on the composited, the newly prepared p-ProH/CMWCNT/GCE was scanned with CV among the potential range of −0.8–2.0 V in pH 5.5 PBS (0.2 mol L^{-1}) until the emergence of stable CV curves. Finally, the p-ProH/CMWCNT/GCE was washed and dried in air and then stored in the refrigerator when no used. The modification processes of p-ProH/CMWCNT/GCE can be briefly illustrated as Scheme 1 shows.

2.4. Real sample pretreatment

For pharmaceutical preparations, homogenous powder of five BrH tablets was firstly obtained by finely pulverizing in a mortar. The powder was transferred to 100 mL volumetric flask and then methanol was added to the scale line. 10 min of sonication was followed in order to make sure the complete dissolution of BrH. After 10 min of centrifugation on the high speed centrifuge at the speed of 8000 rpm, supernatant with accurate volumes were transferred into the electrochemical cell with 5 mL pH 5.5 PBS (0.2 mol L^{-1}) presented to get pharmaceutical preparation sample solutions. As for human blood serum, insoluble matrixes were firstly removed by 10 min of centrifugation at the speed of 8000 rpm. The supernatants collected were diluted 10 folds with pH 5.5 PBS (0.2 mol L^{-1}) to prepare serum sample solutions. DPV method was employed to determine BrH in real samples and standard addition method was used for recovery study. This study was performed in strict accordance with the Guidelines for Care and Use of Laboratory Animals of Fujian Agriculture and Forestry University, and was approved by the Animal Ethics Committee of the College of Life Sciences, Fujian Agriculture and Forestry University.

3. Results and discussion

3.1. Characterization of the p-ProH/CMWCNT/GCE

3.1.1. FESEM characterization. For the purpose of clarifying the surface morphology of the modified electrode, FESEM technique was adopted and the typical FESEM images of CMWCNT/GCE and p-ProH/CMWCNT/GCE was illustrated in Fig. 2. As shown in Fig. 2(A), the PVA-dispersed CMWCNT are evenly distributed on the surface of the electrode and show a distinct tubular structure. While after the electropolymerization of p-ProH film on the CMWCNT/GCE (Fig. 2(B)), the microstructure of the electrode surface has changed significantly. The original tube gaps were filled with certain substances and the voids between the nanotubes became smaller, indicating the successful deposition of p-ProH film at the periphery of CMWCNT. In order to certify the consistency of the p-ProH/CMWCNT/GCE surface after BrH sensing, an independent modified electrode was prepared simultaneously and its surface morphology was recorded after electrochemical test. The result shows that the electrode surface morphology did not

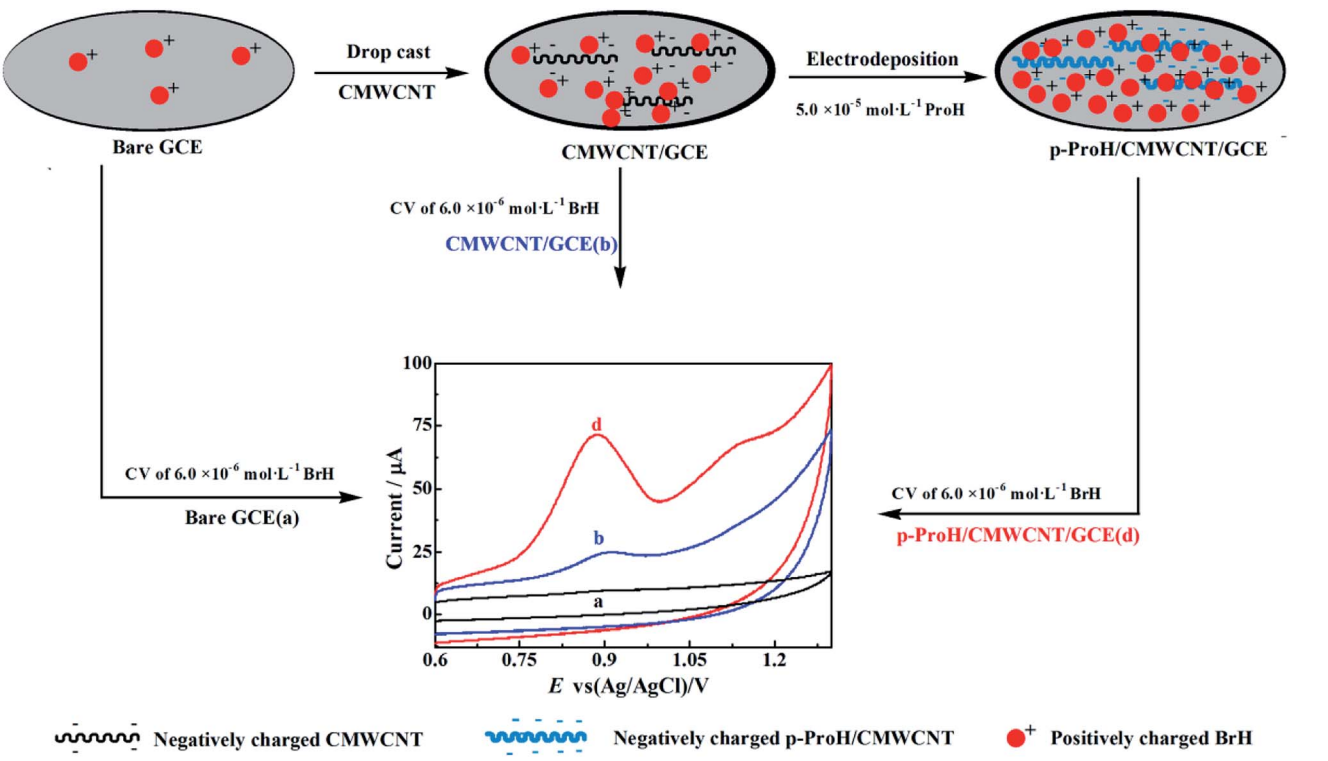

Scheme 1 The fabrication process of the p-ProH/CMWCNT/GCE.

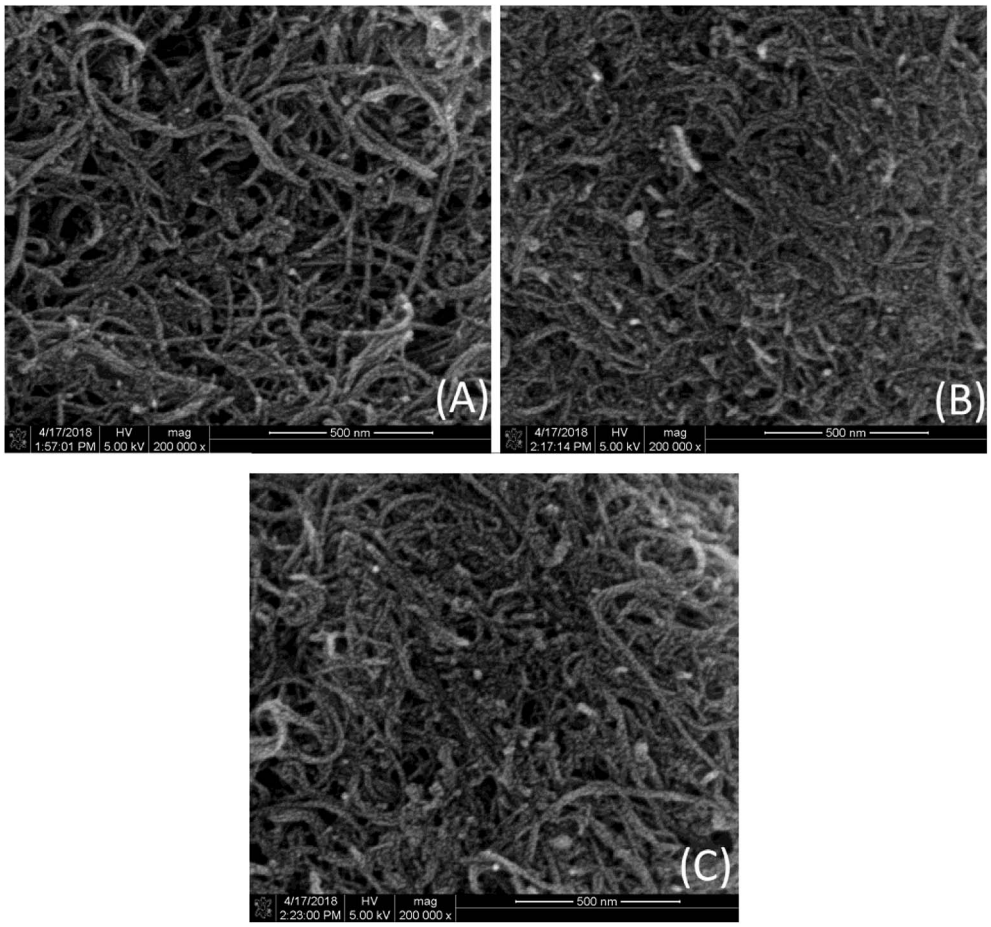

Fig. 2 The typical FESEM images of CMWCNT/GCE (A) and p-ProH/CMWCNT/GCE before (B) and after (C) the sensing.

change significantly after the electrochemical testing (compared Fig. 2(B) and (C)).

3.1.2. EIS characterization. Electrochemical impedance spectroscopy (EIS) technique is an effective means to characterize the electron transfer efficiency on the electrode surface and is usually represented in the form of Nyquist curve which gives a straight line in the low frequency range and a semicircle in the high frequency range. The diameter of the semicircle in the high frequency range represents the charge-transfer resistance (R_{ct}) between the self-assembled membrane and the electrode surface.[35] Fig. 3 shows the Nyquist curves and the corresponding Randle's equivalent circuit model used to fit the impedance data of different electrodes in the 10 mmol L^{-1} $K_3Fe(CN)_6/K_4Fe(CN)_6$ containing 0.1 mol L^{-1} KCl. From curve a, a clear semicircle could be observed at high frequency range for bare GCE and R_{ct} value of 440 Ω was obtained. When CMWCNT or p-ProH was modified on the GCE, the semicircles at high frequency range significantly reduced (curves b and c) and the R_{ct}s values of 133 Ω and 92 Ω were gotten at CMWCNT/GCE and p-ProH/GCE, respectively. This results can be ascribed to the excellent electron transfer efficiency of CMWCNT and p-ProH film. The disappearance of the semicircle at high frequency range on the Nyquist curve of p-ProH/CMWCNT/GCE reflecting the

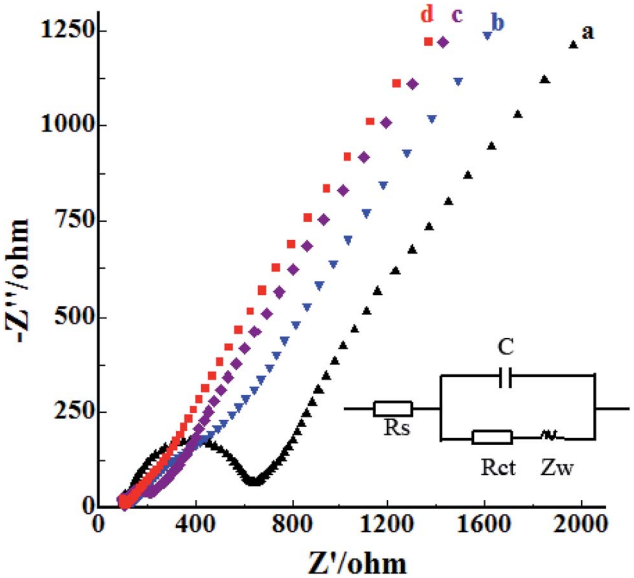

Fig. 3 The Nyquist curves for different electrodes in the 10 mmol L^{-1} $K_3Fe(CN)_6/K_4Fe(CN)_6$ containing 0.1 mol L^{-1} KCl. (a) GCE; (b) CMWCNT/GCE; (c) p-ProH/GCE; (d) p-ProH/CMWCNT/GCE. Inset: Randles equivalent circuit model.

extremely high electron conduction efficiency of the composite membrane modified electrode, and the corresponding R_{ct} value was further decreased to 20 Ω. The above experimental results indicate that the CMWCNT and p-ProH membranes have a synergistic effect on the modified electrode, giving the as prepared modified electrode an extremely high electron conductivity.

3.2. Electrochemical behavior of BrH on the p-ProH/CMWCNT/GCE

In order to elucidate the excellent performance of the p-ProH/CMWCNT composite modified GCE on the electro-oxidation process of BrH, the cyclic voltammetric (CV) curves of 6×10^{-6} mol L^{-1} BrH at different electrodes in the potential range of 0.6–1.3 V were recorded and shown in Fig. 4. As Fig. 4 shows, the CV cure of BrH at the unmodified GCE (Curve a) gives a less obvious oxidation peak at the potential of +0.90 V, which can be ascribed to the first step oxidation of the tertiary amine group in BrH molecules.[10] The minimum oxidation peak current indicates that the electronic transfer rate at the unmodified GCE is very slack, thus the sensitive electrochemical detection of BrH at the bare GCE is impossible. Thanks to the excellent electron conduction efficiency of CMWCNT and p-ProH film, the oxidation peak currents of BrH at the CMWCNT/GCE (Curve b) and p-ProH/GCE (Curve c) are both enhanced. The enhanced peak currents indicates that both CMWCNT and p-ProH film play a good role in the electrochemical oxidation of BrH. Compared curves c and b, we can also find that the oxidation peak current of BrH on p-ProH/GCE is slightly higher than that on CMWCNT/GCE, consisting with the EIS studying result that the R_{ct} of p-ProH/GCE (92 Ω) is slightly less than of CMWCNT/GCE (133 Ω). It is exciting that on the p-ProH/CMWCNT composite film modified GCE, the oxidation peak of BrH at +0.90 V (Curve d) has a significant enhancement compared with CMWCNT/GCE and p-ProH/GCE. This phenomenon should be attributed to the synergistic effect of p-ProH and CMWCNT in the composite film. Compared with p-ProH film modified GCE, the as prepared p-ProH/CMWCNT composite film modified GCE possesses two advantages: firstly, the existence of CMWCNT can provide more modification surface for the electrodeposition of the p-ProH film, providing the composite modified GCE a much larger electro-active surface area; secondly, because the electrons involved in the electrochemical process of the analyte are transported through the electrode interface, CMWCNT can also provide a more efficient transmission interface than the bare GCE. Therefore, p-ProH and CMWCNT can produce synergistic effect on the composite membrane modified electrode, which makes the oxidation peak current of BrH greatly enhanced, bringing favorable conditions for highly sensitive detection of BrH on the composite membrane modified electrodes.

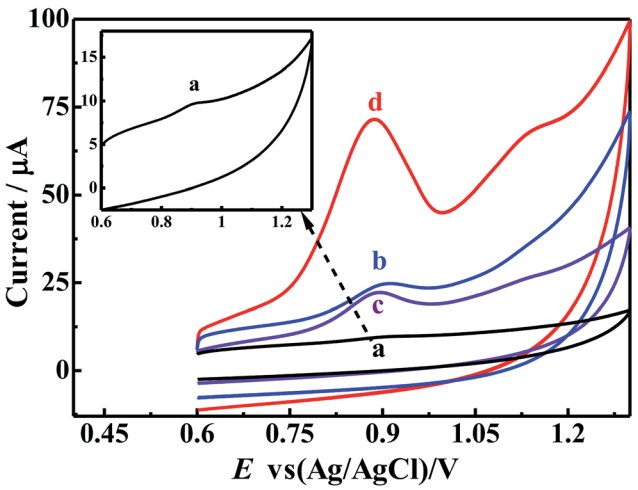

Fig. 4 Cyclic voltammograms of 6×10^{-6} mol L^{-1} BrH in 0.2 mol L^{-1} PBS (pH 5.5) at the bare GCE (a), CMWCNT/GCE (b); p-ProH/GCE (c) and p-ProH/CMWCNT/GCE (d). Initial potential: 0.6 V; final potential: 1.3 V; accumulation time: 8 min; scan rate: 100 mV s^{-1}.

3.3. The influence of scan rate

To investigate the influence of scan rate on the electrochemical behavior of BrH on the p-ProH/CMWCNT/GCE, the CV curves of 2×10^{-5} mol L^{-1} BrH in 0.2 mol L^{-1} PBS (pH 5.5) were collected when the scan rate was increased from 0.01 to 0.15 V s^{-1}. As shown in Fig. 5(A), with the scan rate increases, the oxidation peak current of BrH also gradually increases. Fig. 5(B) shows a good linear relationship between scan rate (ν) and oxidation peak current (i_p), the linear equation is $i_p = 30.904 + 495.82\ \nu$ (i_p: μA, ν: V s^{-1}), with a linear correlation coefficient of 0.9960. Herein, the linear relationship between the oxidation peak current and the scan rate indicates that the electrooxidation of BrH on p-ProH/CMWCNT/GCE is an adsorption controlled process. In addition, the peak potential (E_p) of the oxidation peak shifts to a positive potential as the scan rate increases. By making the $E_p \sim \ln \nu$ plot (Fig. 5(C)), the linear equation of E_p (V) $= 0.955 + 0.0269 \ln \nu$ ($R = 0.9999$) can be obtained. According to the Laviron equation, for an irreversible oxidation process, the relationship between E_p and ν should follow the following relationship:[36]

$$E_P(V) = E^{0\prime} - \frac{RT}{\alpha nF}\ln - \frac{RTk_s}{\alpha nF} + \frac{RT}{\alpha nF}\ln \nu \quad (1)$$

Here, $E^{0\prime}$ refers to formal standard potential, k_s standard rate constant of the reaction, α the transfer coefficient which is supposed to be 0.5 in a completely irreversible electrochemical process,[37] n the electronic number involved in the electro-oxidation process of BrH, other symbols have their usual physical meaning. Accordingly, the value of n is calculated to be 1.91, which is close to 2. Thus there are two electrons participated in the oxidation process of BrH at the potential of +0.90 V.

3.4. The influence of buffer pH

The influence of buffer pH on the electrochemical behavior of BrH was also investigated by increasing the pH of 0.2 mol L^{-1} PBS from 3.5 to 6.5. As Fig. 6(A) shows, the oxidation peak of BrH shifts toward the negative potential as the pH of the buffer increases, indicating that protons participate in the

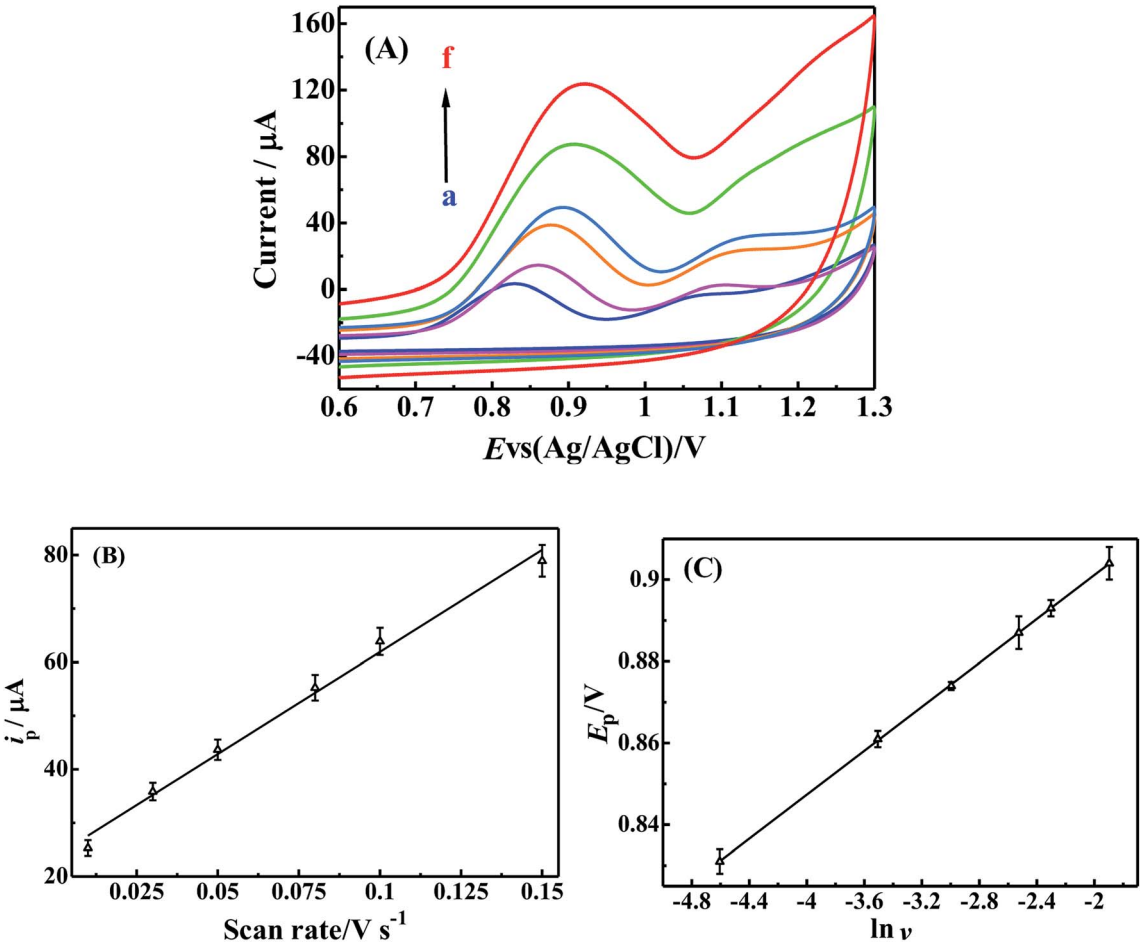

Fig. 5 (A) Cyclic voltammograms of 2×10^{-5} mol L^{-1} BrH at ProH/CMWCNT/GCE under different scan rates (from a to f): 0.01, 0.03, 0.05, 0.08, 0.1, 0.15 V s^{-1} in 0.2 mol L^{-1} PBS (pH 5.5); (B) the relationship between the peak currents and scan rates; (C) the relationship between the peak potential and ln v. Initial potential: 0.6 V; final potential: 1.3 V; accumulation time: 8 min.

electrochemical oxidation of BrH on p-ProH/CMWCNT/GCE. Fig. 6(B) displays the relationship between buffer pH and the corresponding oxidation peak potential (E_p) of BrH, and a linear equation of $E_p = -0.026$ pH + 28.714 ($R = 0.9965$) could be obtained. The slope of the above equation reflects the ratio between the protons number and the electrons number in the electro-oxidation process of BrH. A slope of -0.026 V pH^{-1} is approximately half of -0.059 V pH^{-1}, indicating that the number of protons in BrH oxidation process is half of the electrons number, should be 1. That is, a two-electron and one-proton electrochemical oxidation process occurs in the oxidation of BrH at the potential of +0.90 V, which is consistent with previous reports concerning the electrochemical behavior of BrH.[10,12]

In addition, the pH of the supporting electrolyte also has a significant influence on the oxidation peak current (i_p) of BrH. As Fig. 6(C) shows, in the pH range of 3.5 to 5.5, as the pH increases, the i_p increases continuously. It is worth noting that there is a sudden increase in the i_p value when buffer pH larger than 5.0, this may be related to negatively charged carboxylates group on the p-ProH membrane when pH is higher than 5.0. At this pH, BrH is positively charged due to the protonation, which facilitates the electrostatic adsorption of BrH onto the electrode surface, thus the i_p value abruptly increased. When the pH of the buffer exceeds 5.5, the i_p value begins to decrease, this may be due to the coagulation of BrH in the higher pH medium.[10] In order to obtain the maximum sensitivity in the electrochemical detection of BrH, we chose 5.5 as the buffer pH.

3.5. Optimization of preparation conditions of the modified electrodes

In order to obtain an electrochemical sensor with the highest sensitivity in BrH detection, several preparation conditions such as the CMWCNT volume casted, the concentration of polymer monomer and the number of electropolymerization cycles were optimized by monitoring the i_p value of 2×10^{-5} mol L^{-1} BrH.

1.0, 2.5, 5.0, 7.5 and 10 μL of 2 mg mL^{-1} CMWCNT were used to fabricate the p-ProH/CMWCNT/GCE, separately, to investigated the influence of CMWCNT volume casted. As Fig. 7(A) shows, when 7.5 μL of 2 mg mL^{-1} CMWCNT is casted, the modified electrode gives the highest i_p value. So in the

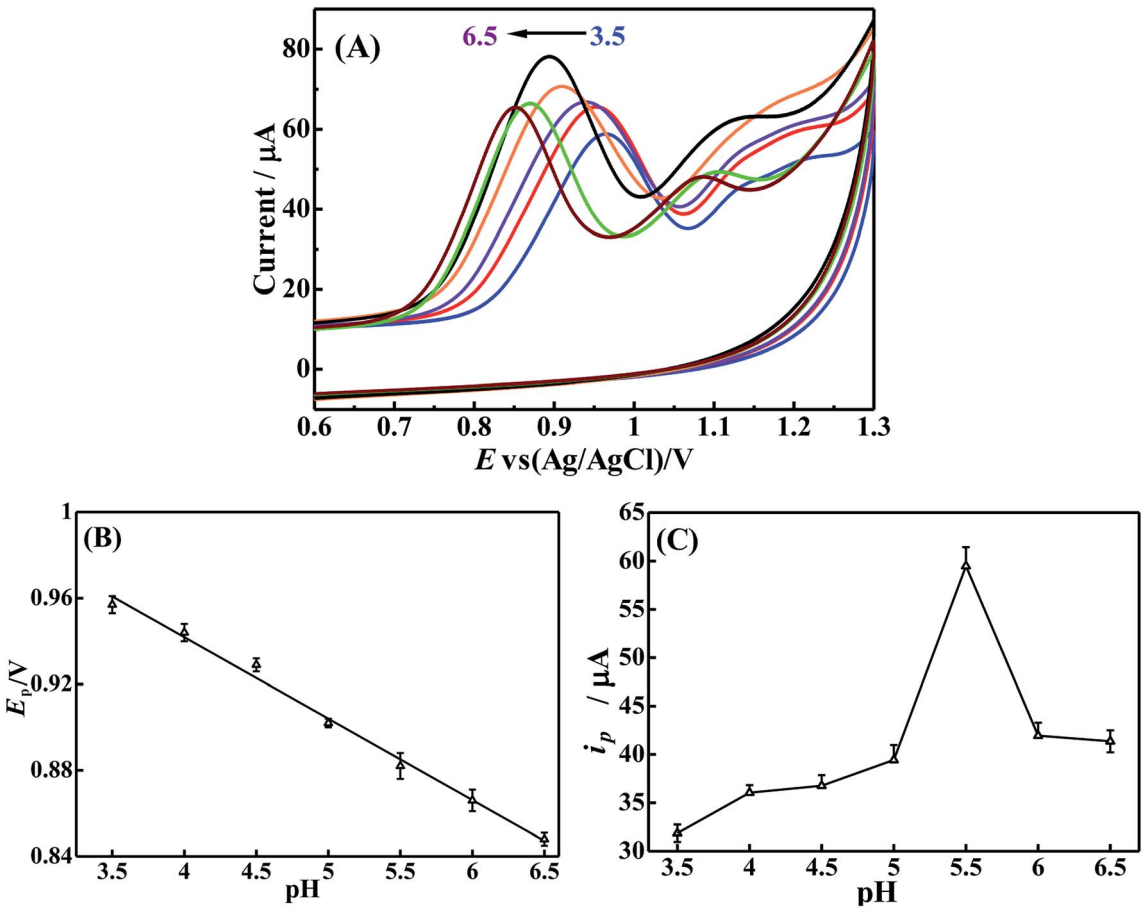

Fig. 6 (A) Cyclic voltammograms of 2×10^{-5} mol L^{-1} BrH at ProH/CMWCNTS/GCE in the 0.2 mol L^{-1} PBS under different pH (from right to left: 3.5, 4.0, 4.5, 5.0, 5.5, 6.0, 6.5); (B) influence of pH on the anode peak potential of BrH; (C) the influence of pH on the peak current of BrH. Initial potential: 0.6 V; final potential: 1.3 V; accumulation time: 8 min; scan rate: 0.1 V s^{-1}.

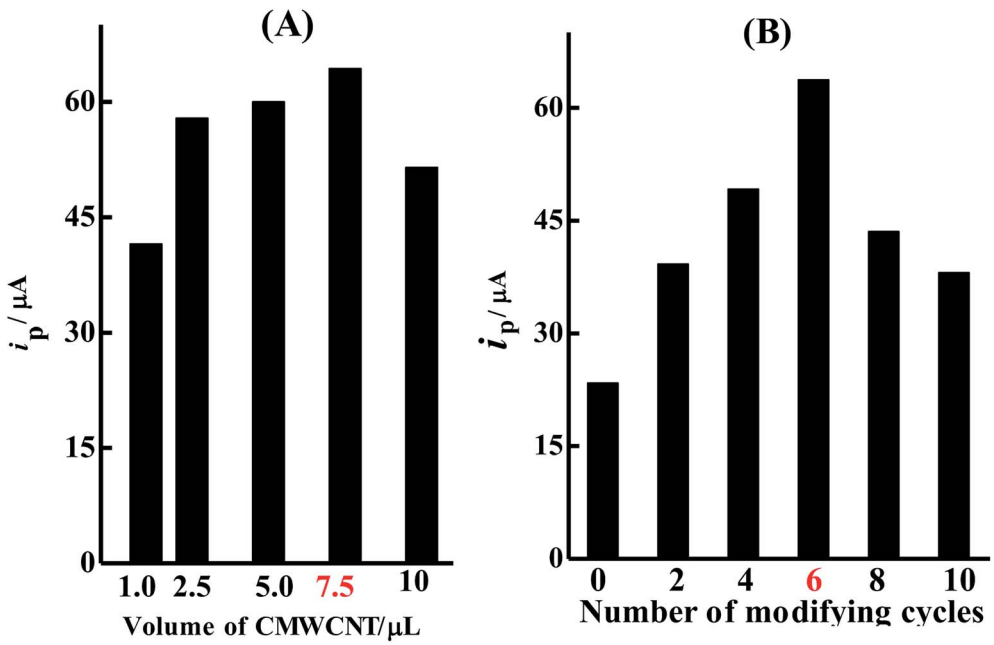

Fig. 7 Effect of CMWCNT volume (A) and modifying cycle (B) on the peak current of BrH.

subsequent experiments, 7.5 μL of 2 mg mL^{-1} CMWCNT is used to fabricated the sensor.

The thickness of the p-ProH film deposited on the modified electrode which depends on the concentration of ProH monomer and electropolymerization cycles has a significant influence on the i_p value of BrH. When the electropolymerization was performed under 6 cycles CV scans, 5 μmol L^{-1}, 10 μmol L^{-1}, 50 μmol L^{-1} and 100 μmol L^{-1} of ProH were used as polymer monomers to prepare the modified electrode. Experiment results revealed that the modified electrode prepared with 50 μmol L^{-1} ProH gave the largest i_p value of BrH (data not shown). Fig. 7(B) shows the influence of the number of electropolymerization cycles on the i_p value of 2×10^{-5} mol L^{-1} BrH when 50 μmol L^{-1} ProH was adopted as the polymer monomer. As can be seen from the figure, the i_p value increases first and then decreases when the number of electropolymerization cycles changed from 0 to 10. When 6 cycles of CV the electropolymerization was performed, the i_p value reaches the maximum. Therefore, p-ProH/CMWCNT/GCE was prepared by 6 CV cycles of electropolymerization in 50 μmol L^{-1} ProH.

3.6. Influence of accumulation time

Our previous report concerning the p-ProH film modified electrode revealed that there are lots of benzene rings and carboxyl groups exist on the p-ProH film,[34] which facilitate the accumulation of BrH on the modified electrode surface. On the one hand, BrH can be adsorbed on p-ProH film by π–π interaction; on the other hand, the carboxyl groups on p-ProH film are negatively charged under the selected pH conditions, and can electrostatically adsorb the positive charge BrH which was protonated. Therefore, the sensitivity can be improved by pre-accumulation of BrH on the modified electrode before electrochemical determination. The effect of accumulation time on the i_p value of 2×10^{-5} mol L^{-1} BrH at p-ProH/CMWCNTS/GCE in 0.2 mol L^{-1} PBS (pH 5.5) was shown in Fig. 8. The results illustrate that the i_p value of BrH increases with the increasing of accumulation time. However, when the accumulation time exceeds 8 minutes, the i_p value almost unchanged over time, indicating that the adsorption of BrH on the electrode surface reaches saturation at 8 minutes. So the optimal accumulation time is 8 min.

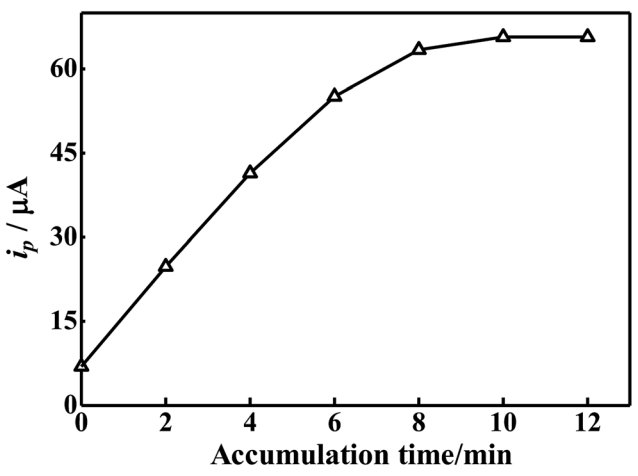

Fig. 8 Effect of accumulation time on the oxidation peak current of 2×10^{-5} mol L^{-1} BrH at p-ProH/CMWCNTS/GCE in 0.2 mol L^{-1} PBS (pH 5.5).

3.7. Analytical characteristics of the modified electrode

Under the above-mentioned optimal conditions, DPV technique was adopted to study the analytical characteristics of the modified electrode in electrochemical detection of BrH. The DPV curves of p-ProH/CMWCNT/GCE in 0.2 mol L^{-1} PBS (pH 5.5) with different BrH concentrations and the corresponding

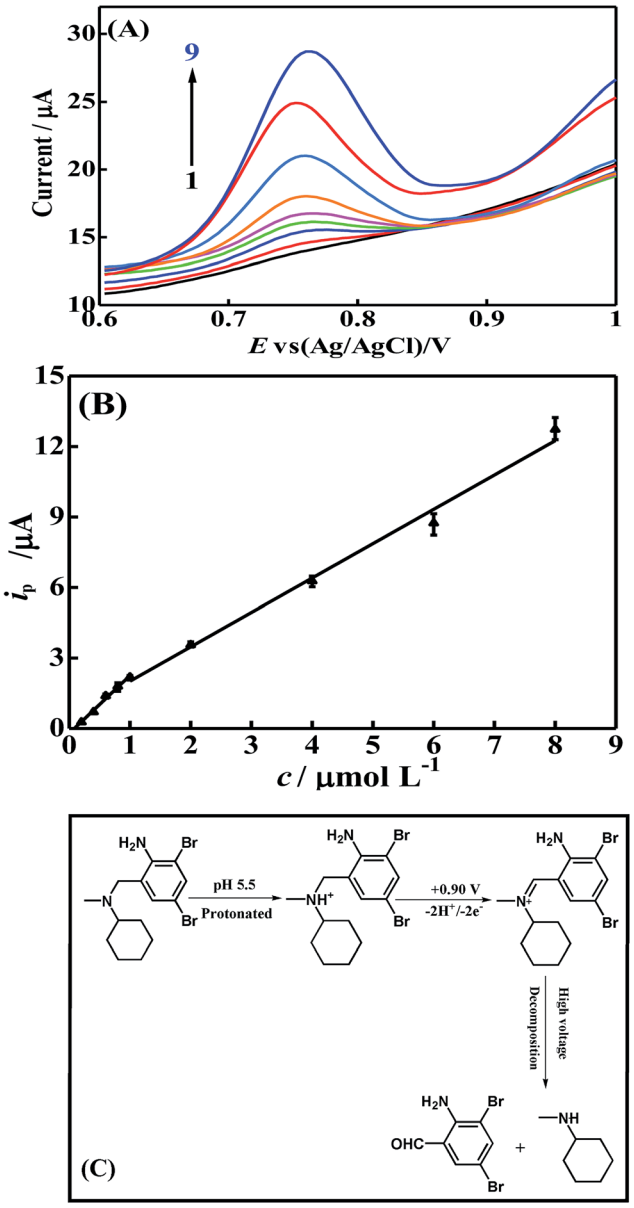

Fig. 9 (A) DPV responses of the p-ProH/CMWCNT/GCE in 0.2 mol L^{-1} PBS (pH 5.5) with different BrH concentrations (1–9: 0.2, 0.4, 0.6, 0.8, 1.0, 2.0, 4.0, 6.0, 8.0 μmol L^{-1} respectively). (B) The calibration curve for the determination of BrH. Initial potential: 0.6 V; final potential: 1.0 V; accumulation time: 8 min. (C) The possible mechanism of the electrochemical oxidation of BrH.

calibration curve were displayed in Fig. 9. From Fig. 9(B) we notice that the proposed electrode exhibits working concentration ranges of 0.2–1.0 μmol L^{-1} and 1.0–8.0 μmol L^{-1} for BrH. The linear regression equation is i_p (μA) = 2.465 c (μmol L^{-1}) − 0.209 (R = 0.9948) and i_p (μA) = 1.463 c (μmol L^{-1}) + 0.553 (R = 0.9956), respectively. The limit of detection (LOD) is calculated to be 0.1 μmol L^{-1} based on signal to noise ratio of 3. The possible mechanism of the electrochemical oxidation of BrH on the modified electrode was shown in Fig. 9(C). In order to prove the superiority of the developed modified sensor in electrochemical determination of BrH, we compared the results of this research with the literature reported electrochemical method, and the comparison results are shown in Table 1. From the data listed in Table 1, we can clearly see that the new developed p-ProH/CMWCNTS composite film modified electrode can provide a lowest detection limited in the electrochemical determination of BrH.

3.8. Reproducibility, repeatability, stability and interferences study

In order to evaluate the reproducibility of the fabricated sensor, we made five independent electrodes at the same time and their i_p response to 2 × 10^{-5} mol L^{-1} BrH were collected. Results showed that the RSD of the i_p responses of the five electrodes was 3.6% (Fig. S1(A)†), indicating the excellent reproducibility in fabricating the p-ProH/CMWCNT/GCE. One electrode was used to ten consecutive DPV measurement of 2 × 10^{-5} mol L^{-1} BrH, the obtained ten i_p values gave a RSD of 5.3% (Fig. S1(B)†), showing that the p-ProH/CMWCNT/GCE was not easy to be contaminated by the redox products in BrH determination, and the modified electrode possesses good repeatability. After DPV measurement of 2 × 10^{-5} mol L^{-1} BrH, the p-ProH/CMWCNT/GCE was carefully washed with water and stored in the refrigerator. The i_p responses of the modified electrode to 2 × 10^{-5} mol L^{-1} BrH remained 98.4%, 95.1% and 91.2% of the initial value after 1, 2, and 3 weeks later, respectively, reflecting good long-term stability of the electrode (Fig. S1(C)†).

In order to employ the as prepared electrode in the quantitative analysis of BrH in real samples such as pharmaceutical preparations and biological fluids, the interferences of common coexisting substances in real samples were studied. Experimental results (Fig. S2†) demonstrated that in DPV measurement of 2 × 10^{-5} mol L^{-1} BrH, the existence of 500 folds concentration of citric acid, magnesium chloride and magnesium stearate, 250 folds concentration of sucrose, glucose, fructose, maltose and lactose, 10 folds concentration of dopamine, ascorbic and uric acid, will not cause obvious change in i_p value (less than ±5%).

3.9. Real sample analysis

The utility of modified electrode in the determination of BrH in pharmaceutical preparations was firstly evaluated. After simple pretreatment as described in Section 2.4, 2.5 μL, 5 μL, 25 μL of the supernatant was accurately transferred into 5 mL pH 5.5 PBS (0.2 mol L^{-1}), to get pharmaceutical preparation sample solutions with three different concentrations (0.49, 0.97, 4.85 μmol L^{-1} according to the marked content). Then DPV technique and standard curve method was used to BrH determination, and the results were illustrated in Table 2. The results show that the detection value is very close to the concentration calculated from the marked content. In order to ensure the reliability of the results, recovery study was conducted using the standard addition method, and the recoveries of 99.0–99.6% were listed in Table 2 concurrently.

Taking serum as real sample, the practicability of the modified electrode in complex samples was also validated. Determination results of three parallel serum samples show that there is no BrH in normal human serum. To verify whether the matrix in the serum will disturb the determination of BrH, three different concentration of BrH were added into the parallel serum samples and the found results were shown in

Table 1 Comparison between the previous literature electrochemical methods for the determination of BrH with the proposed method

Method	Linear dynamic range (μmol L^{-1})	Limit of detection (μmol L^{-1})	Samples analyzed	Reference
DPV	20–100	14	Pharmaceutical preparations	10
FIA-ED	0.31–2.0	0.31	Pharmaceutical preparations	11
NiNPs/MWCNTs/Pt	5–230	3.0	Pharmaceutical preparations	12
p-ProH/CMWCNT/GCE	0.2–1.0 and 1.0–8.0	0.1	Pharmaceutical preparations and human serum	This work

Table 2 Analysis of BrH in pharmaceutical preparations at the fabricated sensor

Concentration level (μmol L^{-1})	Detection results [a] (μmol L^{-1})	R.S.D. (%)	Added (μmol L^{-1})	Found [a] (μmol L^{-1})	Recovery (%)
0.49	0.46	1.3	0.5	0.48	96.0
0.97	0.95	1.2	1.0	0.97	97.0
4.85	4.97	1.6	5.0	4.98	99.6

[a] Values reported are mean of five replicates (n = 5).

Table 3 Analysis of BrH in human serum at the fabricated sensor

Sample	Detection results (μmol L^{-1})	Added (μmol L^{-1})	Found [a] (μmol L^{-1})	Recovery (%)
I	0	0.5	0.51	102
II	0	1.0	0.96	96
III	0	5.0	4.95	99

[a] Values reported are mean of five replicates ($n = 5$).

Table 3. The recovery of 102%, 96% and 99% for three added concentration revealed that the matrix effect in serum would not disturb the detection of BrH.

4. Conclusion

To exert the synergistic effect of p-ProH polymer film and CMWCNT, we fabricated p-ProH/CMWCNT composite modified glassy carbon electrode for the first time. Due to the excellent electronic conductivity of p-ProH film and CMWCNT, together with the accumulation effect of p-ProH film on BrH, the as prepared modified electrode exhibits high sensitivity in the electrochemical determination of BrH. Compared with the literatures reported electrochemical method, the detection limit of BrH in this reported method is effectively reduced. The electrode showed good reproducibility and anti-interference ability in the electrochemical determination of BrH, and it has been successfully applied to the analysis of BrH in pharmaceutical preparations and simulated human serum sample.

Conflicts of interest

There are no conflicts to declare.

Acknowledgements

The authors gratefully acknowledge the support of this work by the Undergraduate Innovative Training Program of Fujian Agriculture and Forestry University and the Test Center of Fuzhou University for FESEM characterization.

References

1 H. O. Ammar and S. A. el-Nahhas, *Pharmazie*, 1995, **50**, 408–410.
2 A. C. B. Dias, J. L. M. Santos, J. Lima and E. A. G. Zagatto, *Anal. Chim. Acta*, 2003, **499**, 107–113.
3 R. A. Khalil and A. M. A. Saeed, *J. Chin. Chem. Soc.*, 2007, **54**, 1099–1105.
4 I. H. I. Habib, M. E. M. Hassouna and G. A. Zaki, *Farmaco*, 2005, **60**, 249–254.
5 M. Javanbakht, M. H. Namjumanesh and B. Akbari-Adergani, *Talanta*, 2009, **80**, 133–138.
6 P. M. Njaria, K. O. Abuga, F. N. Kamau and H. K. Chepkwony, *Chromatographia*, 2016, **79**, 1507–1514.
7 E. Sumarlik and G. Indrayanto, *J. Liq. Chromatogr. Relat. Technol.*, 2004, **27**, 2047–2056.
8 M. Pospisilova, M. Polasek and V. Jokl, *J. Pharm. Biomed. Anal.*, 2001, **24**, 421–428.
9 Q. Jiang, F. Nie and J. Lu, *Luminescence*, 2008, **23**, 32–36.
10 M. Turchan, P. Jara-Ulloa, S. Bollo, L. J. Nunez-Vergara, J. A. Squella and A. Alvarez-Lueje, *Talanta*, 2007, **73**, 913–919.
11 J. Mika, J. C. Moreira, A. Nemeckova, J. Zima, J. Barek and H. Dejmkova, *Monatsh. Chem.*, 2015, **146**, 1211–1215.
12 A. Kutluay and M. Aslanoglu, *Sens. Actuators, B*, 2014, **192**, 720–724.
13 Q. Hao, J. Pang, Y. Zhang, J. Wang, L. Ma and O. G. Schmidt, *Adv. Opt. Mater.*, 2018, **6**, 1700984.
14 K. Wang, J. Pang, L. Li, S. Zhou, Y. Li and T. Zhang, *Front. Chem. Sci. Eng.*, 2018, **12**, 376–382.
15 J. B. Pang, A. Bachmatiuk, Y. Yin, B. Trzebicka, L. Zhao, L. Fu, R. G. Mendes, T. Gemming, Z. F. Liu and M. H. Rummeli, *Adv. Energy Mater.*, 2018, **8**, 1702093.
16 K. Olszowska, J. Pang, P. S. Wrobel, L. Zhao, H. Q. Ta, Z. Liu, B. Trzebicka, A. Bachmatiuk and M. H. Rummeli, *Synth. Met.*, 2017, **234**, 53–85.
17 D. Kong, L. Jiang, Y. Liu, Z. Wang, L. Han, R. Lv, J. Lin, C.-H. Lu, Y. Chi and G. Chen, *Talanta*, 2017, **174**, 436–443.
18 N. Aydemir, J. Malmstrom and J. Travas-Sejdic, *Phys. Chem. Chem. Phys.*, 2016, **18**, 8264–8277.
19 M. Ates, *Mater. Sci. Eng., C*, 2013, **33**, 1853–1859.
20 H. C. Budnikov, G. A. Evtugyn and A. V. Porfireva, *Talanta*, 2012, **102**, 137–155.
21 M. M. Barsan, M. E. Ghica and C. M. A. Brett, *Anal. Chim. Acta*, 2015, **881**, 1–23.
22 W. Lei, W. Si, Y. Xu, Z. Gu and Q. Hao, *Microchim. Acta*, 2014, **181**, 707–722.
23 K. Wang, S. Zhou, Y. Zhou, J. Ren, L. Liwei and Y. Lan, *Int. J. Electrochem. Sci.*, 2018, **13**, 10766–10773.
24 J. Pang, A. Bachmatiuk, I. Ibrahim, L. Fu, D. Placha, G. Simha Martynkova, B. Trzebicka, T. Gemming, J. Eckert and M. H. Ruemmeli, *J. Mater. Sci.*, 2016, **51**, 640–667.
25 I. Ibrahim, J. Kalbacova, V. Engemaier, J. Pang, R. D. Rodriguez, D. Grimm, T. Gemming, D. R. T. Zahn, O. G. Schmidt, J. Eckert and M. H. Ruemmeli, *Chem. Mater.*, 2015, **27**, 5964–5973.
26 E. Eksin, G. Bolat, F. Kuralay, A. Erdem and S. Abaci, *Polym. Bull.*, 2015, **72**, 3135–3146.
27 H. V. Tran, B. Piro, S. Reisberg, L. D. Tran, H. T. Duc and M. C. Pham, *Biosens. Bioelectron.*, 2013, **49**, 164–169.

28 S. Yang, L. Li, X. Zhang, P. Shang, S. Ding, W. Zha and W. Xu, *Can. J. Chem.*, 2017, **95**, 799–805.
29 M. Kesik, F. E. Kanik, J. Turan, M. Kolb, S. Timur, M. Bahadir and L. Toppare, *Sens. Actuators, B*, 2014, **205**, 39–49.
30 N. Hui, F. Chai, P. Lin, Z. Song, X. Sun, Y. Li, S. Niu and X. Luo, *Electrochim. Acta*, 2016, **199**, 234–241.
31 K. Rajalakshmi and S. A. John, *Sens. Actuators, B*, 2015, **215**, 119–124.
32 M. B. Wayu, L. T. DiPasquale, M. A. Schwarzmann, S. D. Gillespie and M. C. Leopold, *J. Electroanal. Chem.*, 2016, **783**, 192–200.
33 L. Yang, J. Yang, B. Xu, F. Zhao and B. Zeng, *Talanta*, 2016, **161**, 413–418.
34 D. Kong, Q. Zhuang, Y. Han, L. Xu, Z. Wang, L. Jiang, J. Su, C.-H. Lu and Y. Chi, *Talanta*, 2018, **185**, 203–212.
35 M. Muti, A. Erdem, A. Caliskan, A. Sınag and T. Yumak, *Colloids Surf., B*, 2011, **86**, 154–157.
36 E. Laviron, *J. Electroanal. Chem. Interfacial Electrochem.*, 1979, **101**, 19–28.
37 Y. Lin, K. Liu, C. Liu, L. Yin, Q. Kang, L. Li and B. Li, *Electrochim. Acta*, 2014, **133**, 492–500.